Unusually high vacancy concentrations in Ni_3Sb

1996 J. Phys.: Condens. Matter 8 7689

(http://iopscience.iop.org/0953-8984/8/41/014)

J. Phys.: Condens. Matter **8** (1996) 7689–7698. Printed in the UK

Unusually high vacancy concentrations in Ni_3Sb

O G Randl†, G Vogl‡, M Kaisermayr‡, W Bührer§, J Pannetier† and W Petry‖

† Institut Laue–Langevin, BP 156X, F-38042 Grenoble Cédex 9, France
‡ Institut für Festkörperphysik der Universität Wien, Strudlhofgasse 4, A-1090 Wien, Austria
§ Labor für Neutronenstreuung, Paul-Scherrer-Institut, CH-5232 Villigen PSI, Switzerland
‖ TU München, Physik-Department E13, James-Franck-Straße, D-85748 Garching bei München, Germany

Received 7 May 1996

Abstract. The structure of the intermetallic alloy Ni_3Sb (the high-temperature phase) has been studied by means of neutron diffraction. Alloys with Ni contents between 71 and 75 at.% were examined at temperatures ranging from 600 to 1000 °C. The results confirm DO_3 structure as well as the existence of vacancy concentrations of up to 20% of the Ni sites. The high number of vacancies certainly plays a crucial role in stabilizing the DO_3 phase; it is also held responsible for the extraordinarily high Ni diffusivity values found in tracer diffusion studies.

1. Introduction

Intermetallic alloys are characterized by the strong bonding forces between their constituents, which are responsible for their strength and high degree of order. One would expect the atomic mobility in such alloys to be very low, but the alloys Fe_3Si, and Ni_3Sb of DO_3 structure (see figure 1; space group: $Fm\bar{3}m$) have been shown to possess astonishingly high diffusivities (Fe_3Si: Sepiol and Vogl (1993); Ni_3Sb: Heumann and Stüer (1966), Sepiol *et al* (1994), Vogl *et al* (1996)). Ni_3Sb is a particularly interesting case, for the Ni atoms of this alloy possess the highest mobility ever observed in a metallic system! What is the reason for this surprising fact?

We have studied diffusion in different DO_3 alloys. The elementary diffusion jump of the Fe atoms in Fe_3Si has been determined using quasi-elastic Mössbauer spectroscopy (QMS): in the stoichiometric alloy the Fe atoms perform nearest-neighbour jumps between α- and γ-sites. Quasielastic neutron scattering (QNS) has shown the same mechanism to be operative in Ni_3Sb (Sepiol *et al* 1994, Vogl *et al* 1996). Therefore, an exotic jump mechanism cannot lie at the origin of fast diffusion in these two compounds. Phonon studies on both alloys (Randl 1994, Randl *et al* 1995, 1996) have allowed us to exclude 'phonon enhancement'—which is responsible for fast diffusion in some group IV metals (Petry *et al* 1989)—as the main reason for the high self-diffusivities.

The hypotheses based on dynamical properties of the alloys (i.e. the diffusion mechanism and phonon enhancement) having been invalidated, one might think that the key to fast diffusion in these intermetallics is linked to their structure. In fact, there is some indication that the vacancy concentration in these alloys is high: Heumann and Stüer (1966) measured the densities of quenched Ni_3Sb alloys of different compositions and compared them to high-temperature x-ray densities. This comparison suggested a high concentration of

0953-8984/96/417689+10$19.50

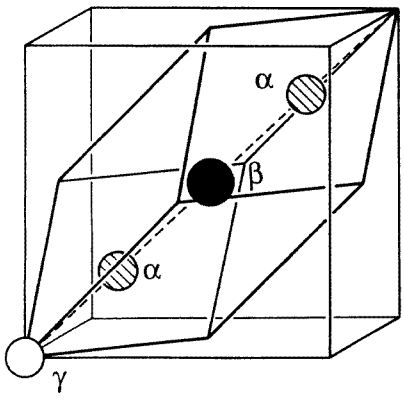

Figure 1. The primitive unit cell of the DO_3 structure: there are four atoms on the three symmetrically different sites of the cell, aligned equidistantly along the cubic space diagonal. In the case of an ideally ordered crystal of composition A_3B, the α- and γ-sites are occupied by A atoms, the β-sites by B atoms.

structural vacancies in the high-temperature phase. It is problematic to conclude on thermal equilibrium properties from quenched samples, but there is additional evidence from positron annihilation measurements that DO_3 alloys tend to contain high vacancy concentrations: Schaefer *et al* (1990) and Kümmerle *et al* (1995) have studied Fe_3Al and Fe_3Si and found high thermal vacancy concentrations. Unfortunately, these measurements only give lower limits for the vacancy concentration if the latter exceeds 0.1 at.%.

A real proof of extraordinarily high vacancy concentrations was discovered in neutron powder diffraction studies on Ni_3Sb compounds of different alloy compositions. Before we describe these experiments and their results, we shall briefly review the literature data concerning Ni_3Sb.

2. Structural knowledge on Ni_3Sb

The Ni-rich high-temperature phase of the Ni–Sb phase diagram—which we will call Ni_3Sb and which is sometimes also referred to as β-phase—was first identified by Lossew in 1906. Although its existence was never doubted, the actual structure of this phase is highly controversial: first x-ray diffraction studies (Fürst and Halla 1938, Osawa and Shibata 1940) gave a tetragonal structure, which was refuted by Schubert (1956) who claimed a cubic (DO_3) phase. Panteleimonov *et al* (cited by Shunk 1969) found a hexagonal cell, whereas Naud and Parijs (1972) reconfirmed Fürst and Halla's findings.

Our measurements—being the first neutron diffraction experiments on Ni_3Sb—should clarify the situation: x-ray diffraction only probes the heavy Sb atoms, whereas neutrons predominantly 'see' Ni ($b_{Ni} = 10.3$ fm; $b_{Sb} = 5.6$ fm).

3. Samples and experimental details

The samples in use have different origins: a first powder sample of the nominal composition $Ni_{72.5}Sb_{27.5}$ (sample A) was produced by one of the authors (OGR) by melting a mixture of high-purity Ni and Sb grains in an induction furnace (under a high-purity argon atmosphere)

Table 1. Nominal Ni content and analysis results for the different alloys examined in the diffraction experiments.

Sample	Nominal concentration (at.% Ni)	Result of analysis (at.% Ni)
A-1	72.5	72.2 ± 0.5
B-1	73	72.7 ± 1.0
B-2	74	73.6 ± 1.0
C-1	71	69.9 ± 1.0
C-2	72	70.4 ± 1.0
C-3	73	71.7 ± 1.0
C-4	74	73.2 ± 1.0
C-5	75	—

and subsequently crushing the alloy rod, the procedure being repeated twice (Randl 1994). The excellent homogeneity of the alloy lumps and their compositions were confirmed by microprobe analysis. Finally, the lumps were crunched in a steel mortar. As Ni_3Sb is a very brittle compound, very fine powders were obtained without effort. The samples for the second (sample B) and third (sample C) series of measurements were prepared at the University of Vienna by B Sepiol and one of the authors (MK), respectively. The alloying techniques were similar. The alloy concentration of these alloys was checked by wet-chemical analysis and found to agree reasonably well with the nominal concentration (see table 1). There are several arguments that make us believe that the deviations for the samples C are due to some systematic error of the analysis.

(a) It is unlikely that Ni is lost in the alloying process, as its vapour pressure is much lower than that of Sb.

(b) The results presented below agree well with the phase diagram (Heinrich *et al* 1978) if the nominal concentrations are approximately correct.

(c) The agreement of the results corresponding to samples B and C of the same nominal composition (see below) is satisfying.

Samples B and C were welded into vanadium cylinders in order to avoid evaporation of Sb at high temperatures.

The measurements were carried out on the DMC spectrometer of the Labor für Neutronenstreuung at the Paul-Scherrer-Institut as well as on the D1B spectrometer of the Institut Laue–Langevin. Details on these diffractometers can be found in Schefer *et al* (1990) and Ibel (1994). The samples were measured at room temperature and at different temperatures in the range from 873 to 1273 K. Only the high-temperature results will be given below—the room temperature phases will be presented in a forthcoming article. Samples A and B were examined on the DMC spectrometer, using a wavelength of 1.7 Å, once in the high-resolution set-up (A), and once in the high-flux configuration (B). The samples C were measured on D1B using a wavelength of 2.52 Å. This wavelength is obviously too long to determine the crystal structure with high precision (few peaks are left), but as the structure was clear at this stage, we decided to concentrate on the low-lying peaks. In all of the cases the samples were mounted in a vanadium resistance furnace. During the experiments on DMC, the furnace was rotated in the measuring plane in order to decrease texture effects.

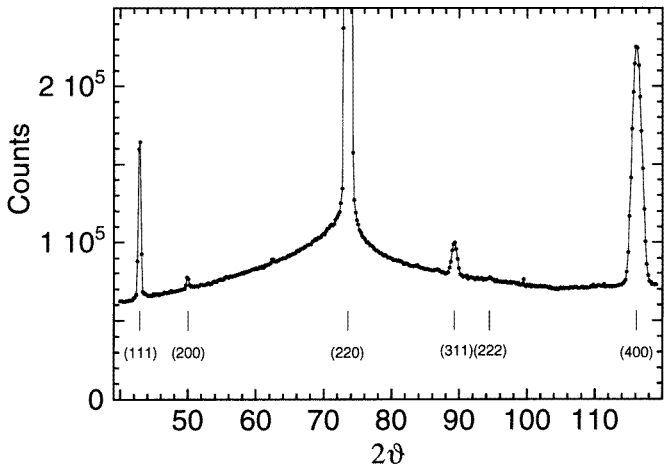

Figure 2. The diffraction pattern of $Ni_{72}Sb_{28}$ at 1073 K, as measured on D1B. The scale has been chosen in such a way that the low-intensity superlattice peaks are visible.

4. Data treatment

For the data treatment the Rietveld fit program FULLPROF (Rodriguez-Carvajal 1994) has been used. The background was interpolated linearly between the points fixed by eye. In the case of the single-phase patterns, typically fitting parameters were refined using the maximum-likelihood method: in particular, the lattice parameter a, and an isotropic temperature factor, as well as the probability of occupation of the different sites.

5. Results

Figure 2 shows one typical diffraction pattern as measured on D1B. Two facts should be noted.

(1) There is no doubt that the structure is cubic. The claims of a tetragonal (Fürst and Halla 1938, Osawa and Shibata 1940, Naud and Parijs 1972) or a hexagonal phase (Panteleimonov *et al*, cited by Shunk 1969) cannot be confirmed. The peak positions correspond to those expected for a DO_3-ordered cubic structure. In fact, this structure gives rise to three classes of peaks:

(a) the 'fundamental peaks' that would remain even if the structure was completely disordered, i.e. bcc; their (hkl) are all even and $h + k + l = 4n$ ($n \in \mathbb{N}$), e.g (220), (400), (422);

(b) the superlattice peaks belonging to B2 order, which is intermediate between DO_3 and bcc order; their (hkl) are all even and $h + k + l = 4n - 2$ ($n \in \mathbb{N}$), e.g (200), (222), (420), ...; and

(c) the superlattice peaks that belong exclusively to DO_3 order; their (hkl) are all odd, e.g. (111), (311), (331) etc.

For the sake of correctness, it should be noted that the classes (b) and (c) are 'superlattice' peaks only with respect to the bcc structure. The fact that all three classes appear in the spectrum shows that DO_3 order is unambiguously established.

One might at first sight be astonished by the strong scattering intensity around the (220) peak, but this is easily understood as thermal diffuse scattering. In fact, the inelastic structure factor for acoustic phonons has a maximum near the 'fundamental' peaks. The thermal nature of this diffuse scattering is corroborated by the fact that room temperature spectra show no such intensity around the corresponding peaks of the low-temperature structure.

(2) It is the relative intensity of the different peaks that gives information on the perfection of order in the system. Of course, there has to be some deviation from ideal DO_3 order as soon as the stoichiometric composition $Ni_{75}Sb_{25}$ is departed from: in $Ni_{72}Sb_{28}$, for example, the excess of Sb atoms has to be compensated, which can be done in three ways:

(a) by placing antistructure Sb atoms on Ni sites;
(b) by placing vacancies on Ni sites; or
(c) by a combination of both (a) and (b).

In order to estimate the consequence for the diffraction pattern, let us have a look at the elastic coherent scattering cross section for an ideal crystal (Squires 1978)

$$\left(\frac{\partial\sigma}{\partial\Omega}\right)_{coh} = N\frac{(2\pi)^3}{V_0}\sum_{h,k,l}|F_{hkl}|^2\delta(\boldsymbol{Q}-\boldsymbol{G}_{hkl}) \tag{1}$$

where N is the number of elementary cells in the crystal, V_0 is the volume of one elementary cell, $|F_{hkl}|^2$ is the squared structure factor (see below), $\boldsymbol{Q}$ is the momentum transfer, and $\boldsymbol{G}_{hkl}$ is a reciprocal-lattice vector. As we are studying powder diffraction results, we have to integrate over all of the orientations of the powder grains. A complete derivation of the count rate of the (hkl) reflection, taking into account the geometry of the detector, yields (Squires 1978)

$$\frac{\Delta I_{hkl}}{\Delta t} = \frac{N\Phi C}{V_0\sin(2\vartheta_{hkl})\sin(\vartheta_{hkl})}|F_{hkl}|^2M_{hkl} \tag{2}$$

where Φ is the incoming flux, c is an instrumental scaling factor, $2\vartheta_{hkl}$ is the scattering angle, and M_{hkl} is the multiplicity of the reflection.

Table 2. The squared structure factors $|F_{hkl}|^2$ (in barns) corresponding to the different possibilities of compensation for the Sb excess in $Ni_{72}Sb_{28}$. The values for ideal DO_3 structure, i.e. $Ni_{75}Sb_{25}$, have been added for comparison. Please note that the multiplicities of the peaks (important for *powder* measurements) are not included.

	(111)	(200)	(220)
Ideal DO_3	0.22	0.22	13.35
Sb atoms on both α- and γ-sites	0.20	0.20	12.95
Sb atoms on α-sites only	0.22	0.17	12.95
Sb atoms on γ-sites only	0.17	0.27	12.95
Vacancies on both α- and γ-sites	0.10	0.10	10.32
Vacancies on γ-sites only	0.00	0.82	10.32
Vacancies on α-sites only	0.22	0.00	10.32

The only quantity that is influenced by structural imperfections is $|F_{hkl}|^2$:

$$|F_{hkl}|^2 = \left|\sum_{m=1}^{N_A} b_m\exp(-W_m(|\boldsymbol{G}_{hkl}|))\exp(\mathrm{i}\boldsymbol{G}_{hkl}\cdot\boldsymbol{d}_m)\right|^2. \tag{3}$$

m sums over the different sites in the elementary unit cell, b_m denotes the coherent scattering length of the atom on site m, and $\boldsymbol{d}_m$ denotes the site position in the unit cell. By inserting the set of $\boldsymbol{d}_m$ for the DO_3 cell and neglecting the Debye–Waller factor $\exp(-W_m(|\boldsymbol{G}_{hkl}|))$ (which is similar for peaks close to each other in reciprocal space), we can write

$$|F_{hkl}|^2_{DO_3} = \left|\sum_{m=1}^{4} b_m \exp\left(\mathrm{i}\frac{\pi}{2}m(h+k+l)\right)\right|^2 . \tag{4}$$

The formula takes this simple form as the four atoms of the primitive unit cell (index m) are aligned along the cubic space diagonal. The order being disturbed, we cannot attribute one sort of atom to each site. Rather,

$$b_m = c^m_{Ni} b_{Ni} + c^m_{Sb} b_{Sb} \tag{5}$$

where c^m_{Ni} and c^m_{Sb} are the concentrations of the Ni and Sb atoms on site m, and b_{Ni} and b_{Sb} are the corresponding scattering lengths. The concentrations have to fulfil the relation

$$c^m_{Ni} + c^m_{Sb} + c^m_V = 1 \tag{6}$$

where c^m_V denotes the vacancy concentration on site m.

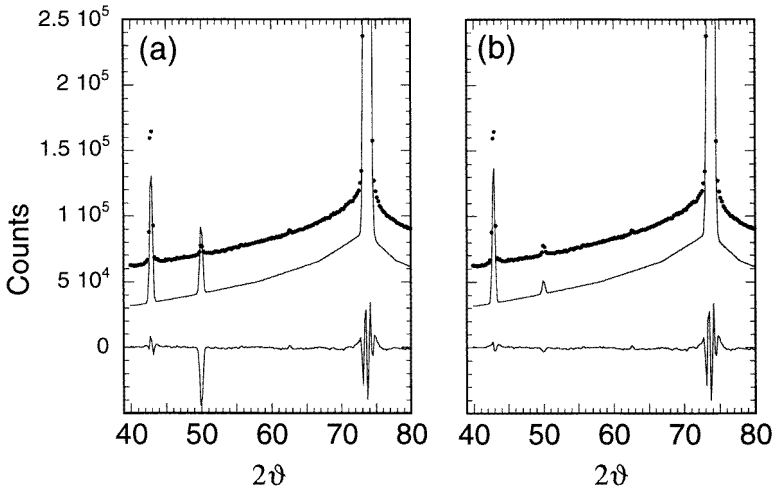

Figure 3. A comparison between the Rietveld fits for $Ni_{72}Sb_{28}$ at 1073 K, assuming (a) Sb antistructure atoms, and (b) vacancies on Ni sites. In order to separate optically the raw data (points) and the fit (full curve), the latter is printed with an artificial offset of 3×10^4 counts. The difference between the fit and the data is plotted at the bottom of the figures. Clearly, only the vacancy model gives a satisfactory fit.

We have seen that the relative intensities in the diffraction spectra should correspond to the squared structure factors of the Bragg peaks (times the multiplicity). Table 2 gives this factor for the different cases of disorder that we consider and the first three peaks of the pattern: (111), (200), and (220).

For an ideal DO_3 structure, the structure factors of (111) and (200) are identical. If we take into account the multiplicity of the peaks (eight for (111) and six for (200)), we expect an intensity ratio $I(200):I(111) = 6{:}8$ for ideal DO_3. From figure 2 we can see that in the measured pattern the intensity of the (200) peak is much lower than expected. The structure is not ideally ordered. Moreover, table 2 tells us that *only* vacancies on α-sites can

explain a significant lowering of the relative intensity of (200). This is also demonstrated in figure 3.

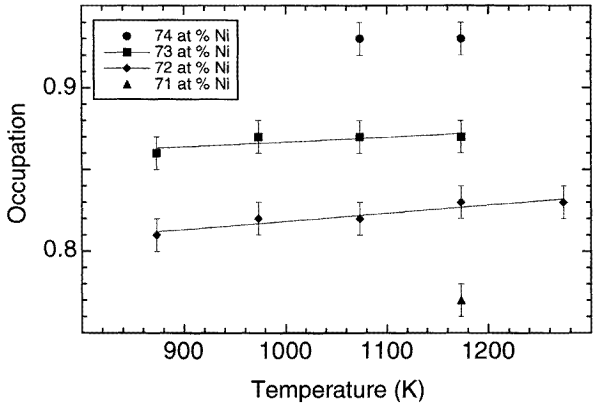

Figure 4. The dependence of the occupation of the α-sites on the temperature and the alloy concentration. Temperatures and alloy concentrations at which a two-phase mixture was found have not been taken into account.

Table 3. Results of the Rietveld fits for all of the measured diffraction patterns. a is the lattice parameter, $B = 16\pi\langle u_\alpha^2\rangle$ is the isotropic displacement parameter, $O(\alpha)$ and $O(\gamma)$ are the occupation probabilities of the α- and γ-sites, and χ^2 is a goodness-of-fit parameter. The errors of the occupation numbers are about three times the errors given by the Rietveld fit. The measurements marked (*) have been carried out on the DMC spectrometer, the others on D1B.

Atomic per cent of Ni	T (K)	a (Å)	B (Å^2)	$O(\alpha)$	$O(\gamma)$	χ^2	Second phase
71	1073	5.8742(4)	5.1(1)	0.80(1)	0.93(1)	1.83	Yes
71	1173	5.8820(4)	5.6(1)	0.77(1)	0.90(1)	2.13	—
72	873	5.8686(4)	5.5(1)	0.81(1)	0.95(1)	2.09	—
72	973	5.8824(4)	5.4(1)	0.82(1)	0.94(1)	2.10	—
72	1073	5.8971(4)	5.8(1)	0.82(1)	0.93(1)	2.01	—
72	1173	5.9097(4)	6.4(1)	0.83(1)	0.92(1)	1.85	—
72	1273	5.9215(5)	7.1(1)	0.83(1)	0.91(1)	2.08	—
72.5 (*)	873	5.8881(3)	2.5(1)	0.82(1)	0.99(1)	5.74	—
73	873	5.9009(4)	5.0(1)	0.86(1)	0.98(1)	2.40	—
73	973	5.9149(4)	5.4(1)	0.87(1)	0.97(1)	2.17	—
73	1073	5.9282(5)	5.8(1)	0.87(1)	0.96(1)	2.41	—
73 (*)	1073	5.9314(3)	5.4(1)	0.87(1)	0.97(1)	2.27	—
73	1173	5.9417(5)	6.2(1)	0.87(1)	0.96(1)	2.25	—
74	1073	5.9435(4)	4.8(1)	0.93(1)	1.00(1)	2.10	Ni
74 (*)	1073	5.9602(3)	4.8(1)	0.92(1)	1.00(1)	2.41	Ni
74	1173	5.9516(5)	5.8(1)	0.93(1)	1.00(1)	2.28	Ni
75	1073	5.9343(4)	5.0(1)	0.92(1)	1.00(1)	2.27	Ni
75	1173	5.9446(4)	5.1(1)	0.92(1)	1.00(1)	1.97	Ni
75	1273	5.9544(5)	5.3(2)	0.92(1)	1.00(1)	2.20	Ni

It turns out that this exemplary case is representative for all of the spectra: reasonable fits of the patterns can only be obtained if vacancies on the Ni sites are introduced. Therefore,

the Rietveld fits have been carried out in the following way: the β-sites were considered to be completely filled with Sb atoms, which automatically determines the sum of the occupation probabilities of the different Ni sites (via the alloy composition!) Initially, all of the vacancies were kept on the α-sites, but during the refinement an exchange of vacancies between α- and γ-sites was allowed. The alloy concentration was superimposed as a boundary condition. Table 3 lists the most important fitting results. Please note that the results of the measurements on different instruments (D1B and DMC) under the same conditions (sample composition, temperature) agree reasonably well. Only the measurement on the alloy of composition $Ni_{72.5}Sb_{27.5}$ at 873 K (DMC in the high-resolution set-up) does not follow the general trend of all the other results from both DMC and D1B. We do not know the reason for the discrepancy, but we think that this result has to be discarded. The reader should also note that there is no change in $O(\alpha)$ and $O(\gamma)$ between 74 and 75 at.% Ni, which is due to the fact that the DO_3 phase is stable only up to Ni concentrations of slightly less than 74 at.%. The only change between 74 and 75 at.% Ni is the volume increase of the secondary (Ni) phase.

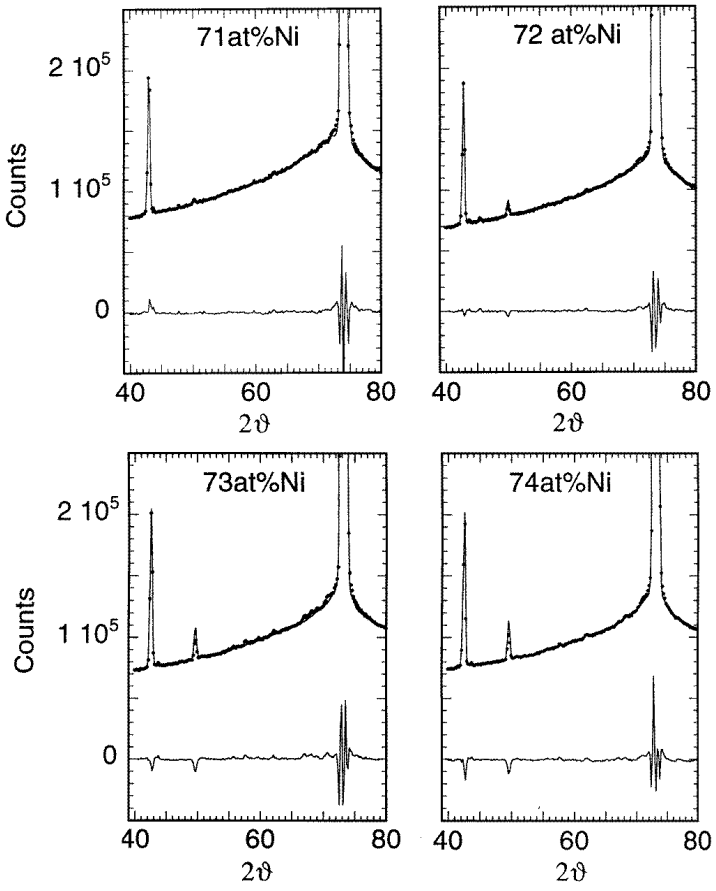

Figure 5. The dependence of the powder pattern of Ni_3Sb at 1173 K as a function of the alloy composition. The raw data (points), the Rietveld fit (full curves), and the difference between them (full curves at the bottom) are shown.

6. Discussion

The following conclusions can be drawn from our results.

(1) The vacancy concentration in the Ni_3Sb alloys is extraordinarily high. This result directly confirms Heumann and Stüer's (1966) guess. Within the precision of the Rietveld fit (about 1 at.% for the occupation probabilities), the Sb excess in the off-stoichiometric alloys is completely made up for by the creation of vacancies on the Ni sites, not by antistructure defects. *Being restrained to the Ni sublattices, the vacancies are 'ordered', which makes them observable via neutron diffraction.*

(2) The temperature dependence (see figure 4) of the vacancy concentration—if there is any—is too small to be ascertained without ambiguity. One might guess a transfer of vacancies from α- to γ-sites with increasing temperature, but this could well be a statistical artefact. Note, however, that the diffraction measurements presented in this paper only allow conclusions to be reached on the relative occupation of the different sites: the diffraction pattern is only changed in *absolute* intensity when the same percentage of vacancies is introduced on all sites of the unit cell. Therefore, we cannot exclude the possibility that thermal vacancies are created isotropically as the temperature increases.

(3) The most distinct result of the present measurements is the very clear dependence of the vacancy concentration on the alloy composition. The effect is clearly visible in the diffraction patterns, as can be seen in figure 5. The higher the Sb content becomes, the greater the number of vacancies created on the Ni sublattices (see also figure 4). These vacancies obviously 'prefer' the α-sublattice, but a considerable number are also found on the γ-sites. The existence of these structural vacancies seems to be crucial for the alloy stability: as soon as there are not enough vacancies to keep some of them in the γ-sublattice (i.e. above 73 at.% Ni), a two-phase mixture ($Ni_3Sb + Ni$) appears.

At the moment, it is unknown why the creation of huge amounts of vacancies (in $Ni_{71}Sb_{29}$ at 1173 K, 19% of the Ni sites are vacant!) is energetically cheaper than the creation of antistructure atoms, but the reason is undoubtedly to be found in the strong Ni–Sb bonding. We strongly suggest *ab initio* calculations to find the answer to this open question. Such calculations have been carried out on the B2 structures NiAl (Fu *et al* 1993, Mayer *et al* 1995) and FeAl (Fu *et al* 1993), but not yet on a DO_3 structure. Ni_3Sb with its anomalously high vacancy concentrations and pronounced composition dependence should be an ideal candidate for such studies.

7. Conclusion

It has been shown that a considerable number of vacancies exist in the DO_3 high-temperature phase of Ni_xSb_{100-x} ($70 < x < 75$). These vacancies are structural, i.e. more or less independent of temperature, and strongly correlated to the relative Sb excess in the alloy. There is no doubt that these high vacancy concentrations are the key to an understanding of the extraordinarily high diffusivity values found in these alloys and to the electronic origin of the phase stability.

Acknowledgments

The authors wish to thank Bogdan Sepiol (University of Vienna) for preparing a series of powder samples. They are also indebted to Andreas Heiming (formerly at the Institut Laue–Langevin, now at Ruhrgas Essen). Financial support from the Austrian Fonds zur

Förderung der wissenschaftlichen Forschung (FWF), project number S5601, is gratefully acknowledged.

References

Fu C L, Ye Y Y, Yoo M H and Ho K M 1993 *Phys. Rev.* B **48** 6712
Fürst U and Halla F 1938 *Z. Phys. Chem.* B **40** 285
Heinrich S, Rexer H U and Schubert K 1978 *J. Less-Common Met.* **60** 65
Heumann T and Stüer H 1966 *Phys. Status Solidi* **15** 95
Ibel K (ed) 1994 *The Yellow Book—Guide to Neutron Research Facilities at the ILL* (Grenoble: Institut Laue–Langevin)
Kümmerle E A, Badura K, Sepiol B, Mehrer H and Schaefer H E 1995 *Phys. Rev.* B **52** R6947
Mayer J, Elsässer C, and Fähnle M 1995 *Phys. Status Solidi* b **191** 283
Naud J and Parijs D 1972 *Mater. Res. Bull.* **7** 301
Osawa A and Shibata N 1940 *Nippon Kinzoku Gakkai-Shi* **4** 362
Petry W, Heiming A, Trampenau J and Vogl G 1989 *Defect Diffus. Forum* **66–69** 157
Randl O G 1994 *PhD Thesis* University of Vienna
Randl O G, Vogl G, Petry W, Hennion B and Bührer W 1996 to be published
Randl O G, Vogl G, Petry W, Hennion B, Sepiol B and Nembach K 1995 *J. Phys.: Condens. Matter* **7** 5983
Rodriguez-Carvajal J 1994 private communication
Schaefer H E, Würschum R, Sob M, Zak T, Yu W Z, Eckert W and Banhart F 1990 *Phys. Rev.* B **41** 11 869
Schefer J, Fischer P, Heer H, Isacson A, Koch M and Thut R 1990 *Nucl. Instrum. Methods* **288** 477
Schubert K 1956 *Naturwissenschaften* **43** 248
Sepiol B, Randl O G, Karner C, Heiming A and Vogl G 1994 *J. Phys.: Condens. Matter* **6** L43
Sepiol B and Vogl G 1993 *Phys. Rev. Lett.* **71** 731
Shunk F 1969 *Constitution of Binary Alloys* suppl 2 (New York: McGraw-Hill)
Squires G L 1978 *Thermal Neutron Scattering* (Cambridge: Cambridge University Press)
Vogl G, Kaisermayr M and Randl O G 1996 *J. Phys.: Condens. Matter* **8** 4727